Research Square

Preprints are preliminary reports that have not undergone peer review.
They should not be considered conclusive, used to inform clinical practice,
or referenced by the media as validated information.

Soil nitrogen availability reveals contrasting and genotype-dependent microbiome assembly strategies in eggplant

Micol Guaschino

micol.guaschino@crea.gov.it

CREA Research Center Viticulture and Enology: CREA Centro di Ricerca Viticoltura e Enologia
https://orcid.org/0000-0001-5821-6013

Laura Toppino
Maria Rosaria Tassone
Giuseppe Leonardo Rotino
Filippo Salamone
Anna Narduzzo
Giordana Cacco
Walter Chitarra
Luca Nerva

Research Article

Keywords: 16S rRNA amplicon sequencing, root endosphere, functional prediction, mesocosms, Actinobacteria, Bacillus

Posted Date: November 10th, 2026

DOI: https://doi.org/10.21203/rs.3.rs-11319580/v1

License: This work is licensed under a Creative Commons Attribution 4.0 International License.
Read Full License

Soil nitrogen availability reveals contrasting and genotype-dependent microbiome assembly strategies in eggplant

Micol Guaschino[1*], Laura Toppino[2*], Maria Rosaria Tassone[2], Giuseppe Leonardo Rotino[2], Filippo Salamone[2] , Anna Narduzzo[1], Giordana Cacco [1], Walter Chitarra[1,3†] & Luca Nerva[1,3,4,5†*]

[1] Council for Agricultural Research and Economics (CREA) – Research Centre for Viticulture and Enology, Via XXVIII Aprile n. 26, 31015 Conegliano (TV), Italy.

[2] Council for Agricultural Research and Economics (CREA) – Research Centre for Genomics and bioinformatics. Via Paullese n. 28, 26836 Montanaso Lombardo (LO), Italy

[3] Institute for Sustainable Plant Protection – National Research Council (IPSP-CNR), Strada delle Cacce 73, 10135 Torino (TO), Italy.

[4] La Viticola SRL, Via Melchiorre Gioia 11, 10121 Torino (TO), Italy.

[5] Department of Genetics, Faculty of Agrisciences, Stellenbosch University, Matieland, 7602, South Africa.

† These authors equally contributed as senior authors

***Corresponding authors details**

Micol Guaschino: micol.guaschino@crea.gov.it; Luca Nerva: luca.nerva@crea.gov.it; Laura Toppino: laura.toppino@crea.gov.it

Abstract

Aims

Plant genotype and nutrient availability are key drivers of root microbiome assembly, yet their relative contribution remains poorly understood in eggplant (*Solanum melongena* L.).

Methods

In this study, root-associated bacterial communities from four eggplant genotypes, grown under contrasting nitrogen regimes, were characterized using a combined culture-dependent and 16S rRNA gene amplicon sequencing approach.

Results

Across all genotypes, Proteobacteria dominated the root microbiome, while host genotype emerged as the primary determinant of bacterial diversity and community structure. Nitrogen availability acted as a secondary but consistent environmental driver, reshaping community composition and promoting the enrichment of Actinobacteriota under fertilized conditions. Genotypes did not differ in whether their microbiomes responded to nitrogen, but rather in the magnitude of community restructuring, revealing a continuum from highly constrained to more plastic microbial assemblages. Notably, one genotype maintained a stable Bacillus-dominated microbiome regardless of nitrogen availability, suggesting strong host-mediated filtering. Predicted functional profiles mirrored taxonomic differences, particularly for nitrogen-cycling and organic matter degradation functions. The integration of culture-dependent isolation generated a representative collection of dominant bacterial taxa, providing a valuable resource for future functional studies.

Conclusions

Overall, these findings demonstrate that eggplant genotype plays a central role in shaping root microbiome assembly and its responsiveness to nutrient availability, highlighting the potential of microbiome-informed approaches for improving nutrient-use efficiency and crop performance.

Keywords:

16S rRNA amplicon sequencing; root endosphere; functional prediction; mesocosms; *Actinobacteria*; *Bacillus*

Introduction

Plants host complex and taxonomically diverse microbial communities across the rhizosphere, root surface and internal tissues, forming integrated plant-microbe systems whose emergent properties cannot be interpreted from the host genome alone (Vandenkoornhuyse et al. 2015). In this perspective, the plant holobiont represents a functional evolutionary and ecological unit in which microbial partners contribute to nutrient acquisition, stress buffering, pathogen suppression, and the overall regulation of plant performance (Nerva et al. 2022a). Root-associated microbiomes are particularly relevant, as roots serve as the primary interface between plants and soil, a dynamic zone where nutrient availability, host metabolism, and microbial competition converge (Bulgarelli et al. 2013). Recent work has emphasized that roots actively shape beneficial microbiome assembly through chemically diverse metabolites, exudates that may act as nutrients, signals or selective filters for specific microbial groups (Uribe-Acosta et al. 2025). Consequently, plant-associated microbial biodiversity is far more than a static descriptor of belowground ecosystems; it represents a dynamic reservoir of functional traits and a pivotal determinant of crop tolerance to environmental stresses, ultimately driving agricultural adaptation, productivity and sustainability (Yu et al. 2022; Sandrini et al. 2022a).

The assembly of root-associated microbiomes is strongly influenced by root-derived resources. Early experimental evidence showed that artificial root exudates can modify bacterial densities, metabolic signatures and community genetic structures in bulk soil and the maize rhizosphere, indicating that soluble organic compounds released by roots are sufficient to redirect microbial community organization (Baudoin et al. 2003). Nitrogen supply can further modify this interaction by altering both root exudation and microbial community structure (Hao et al. 2022). In maize, nitrogen fertilizer rate affected the quantity and composition of root exudates, including sugars,

sugar alcohols and phenolics, and was linked to changes in the rhizosphere microbiome and nitrogen-use efficiency (Zhu et al. 2016). These observations support a model in which nutrient availability influences plant-microbiome interactions both indirectly, by changing plant physiology and rhizodeposition, and directly, by modifying the ecological constraints experienced by microbial taxa (Trivedi et al. 2020; Dastogeer et al. 2020).

Host genetic background is another major factor controlling microbiome assembly (Zhang et al. 2023). Evidence from perennial plant systems indicates that host genotype and plant age can shape both leaf and root microbiomes, reinforcing the idea that plant identity contributes to the selection of associated microbial communities (Wagner et al. 2016). Root architecture can also structure rhizosphere microbial associations by creating spatially heterogeneous physicochemical conditions along the root system and across soil depths (Sandrini et al. 2022b; Galindo-Castañeda et al. 2024). These mechanisms are particularly relevant for crops selected for contrasting physiological traits, because differences in root metabolism, architecture or nutrient acquisition strategies may lead to distinct microbial recruitment patterns from the same soil microbial pool. Less abundant microbial lineages may also contribute to these processes. Acidobacteriota, for example, include major soil and peatland prokaryotes with diverse genomic capacities (Dedysh et al. 2022), while metagenomic analyses at the soil aggregate scale have shown that microbial communities encode functions involved in nitrogen and phosphorus cycling and that organic amendments can influence these functional profiles (Wu et al. 2021).

Eggplant (*Solanum melongena* L.) is an important solanaceous crop worldwide, yet its microbiome, particularly its endophytic bacterial community, remains markedly understudied relative to other major crops. Prior work addressed endophytic fungal communities (Kiran et al. 2025), while root-internal bacterial communities remain poorly explored. Recent comparative

100 work on rice and eggplant rhizospheric bacteriomes identified microbial features linked to
101 Solanum melongena cultivars, underscoring the relevance of rhizosphere research for productivity
102 and sustainability (Mandal et al. 2025). However, how the eggplant root-associated bacterial
103 microbiome relates to host genotype and nitrogen availability remains unexplored, a gap relevant
104 given that nitrogen limits eggplant productivity (Jilani et al. 2008; Mauceri et al. 2021); improving
105 nitrogen-use efficiency requires understanding both plant physiological responses and the
106 microbial assemblages linked to nutrient acquisition (Gralka et al. 2020; Singh et al. 2022).
107 Here, we investigated the bacterial microbiome associated with roots of four cultivated eggplant
108 genotypes previously selected for contrasting nitrogen-use efficiency under two nitrogen regimes.
109 Combining culture-dependent isolation with 16S rRNA gene amplicon profiling, we aimed to
110 characterize the composition of eggplant root-associated and endophytic bacterial communities,
111 establish a culturable isolate collection for long-term preservation, assess the contribution of host
112 genotype to microbial diversity and community structure, and determine how nitrogen availability
113 shapes these assemblages. This approach positions eggplant within the broader plant holobiont
114 concept, addresses a crop-specific knowledge gap, and identifies culturable bacterial resources that
115 could support future defined microbial community (DMC; Koch et al. 2026) approaches to
116 improve plant performance under reduced or optimized nitrogen inputs.
117

118 **Material and methods**

119 *Experimental design and plant growth conditions*

120 Four eggplant (Solanum melongena L.) accessions previously characterized under hydroponic
121 conditions for contrasting nitrogen-use efficiency (NUE) were selected (Mauceri et al. 2020,
122 2021): 305E40, 67/3, AM194 and AM241. In hydroponic and preliminary glasshouse screenings,

AM241 and 305E40 clustered among the most N-use efficient accessions, while AM194 clustered among the inefficient ones. 305E40 and 67-3 showed a milder contrast in low-N response (67-3 being more efficient than 305E40), but were included as parents of a RIL population (Toppino et al. 2020) mapped for over 70 agronomic traits, with different genome sequence versions and ONT-based sequences available (Barchi et al. 2021, Gaccione et al. 2025), making them useful for future NUE QTL mapping.

Greenhouse trials in 2021 and 2022 evaluated NUE performance and productivity of the four accessions under soil-grown conditions. Plants were grown in mesocosms with steam-sterilized soil mixed with sand (1:1, v/v), across three beds each split into two 5.6 m^2 sectors of 16 plants (Figure 1a). All beds received uniform watering and basal P/K fertilization in August, with two N regimes: 0N (0 U N ha^{-1}) and 3N (200 U N ha^{-1}). Nitrogen was supplied mainly as CaNO3 (YaraTera Calcinit; 15.5% total N, 14.4% nitrate N, 1.1% ammoniacal N, 26.3–26.5% CaO, diluted), via eight split fertilizations (30 g/L, applied around each plant's roots) between May and September 2022, matching 100% of the planned 3N dosage. Fruits were harvested from June to September; auxin-based growth regulators were applied twice weekly from May to promote fruit set (Figure 1b). Physiological, phenotypic and growth parameters were recorded throughout the season (Figure 1c).

Ecophysiological and phenotypic measurements

At the end of the growing season (08 September 2022), plants were phenotypically characterized for growth-related traits and photosynthetic performance. Growth and yield traits (plant height, stem diameter, number of fruits, average fruit weight, fruit and stem dry matter) were recorded for 4 plants per genotype × 3 replicates × 2 treatments. Ecophysiological parameters were measured

with an infra-red gas analyzer (IRGA, ADC-LCi T system; Analytical Development Company, BioScientific Ltd., UK): net photosynthesis (Pn), transpiration rate (E), intercellular CO2 concentration (Ci), water use efficiency (WUE = Pn/E) and apparent carboxylation efficiency (iCE = Pn/Ci) were recorded on sunny days between 9:00 and 11:00 am as previously described (Flexas et al. 2011), on two fully developed, non-senescent leaves per plant (4th–5th leaf from the shoot apex; 15 measurements per condition and treatment). Ambient conditions were kept within 1,000–1,200 µmol photons m^{-2} s^{-1}, 27–30 °C and 420–440 ppm CO2. For each parameter, effects of genotype, nitrogen treatment (0N, 3N) and their interaction were tested by two-way ANOVA with Tukey's HSD post-hoc test in R (Nerva et al. 2022b).

Root sampling and microbial endophytes isolation methods

At the end of the experimental period, root samples were collected from all four genotypes under both 0N and 3N conditions, for both culturable microbial community isolation and DNA extraction for culture-independent microbiome characterization (Figure 1d).

For the culturable approach, roots were shaken free of loose soil, washed under sterile conditions, and surface-sterilized (5 min in 1% NaClO, then 3 washes with sterile water) to remove epiphytic contamination; elimination of epiphytic bacteria was confirmed by plating 100 µL of the final rinse water on LB agar. For each genotype, 1 g of root tissue was homogenized in sterile ringer solution (7.2 g sodium chloride, 0.37 g potassium chloride, 0.17 g calcium chloride per liter) using a sterile grinder to release root-associated and endophytic microorganisms. Homogenates were diluted 1:5 in sterile ringer solution for microbial isolation.

Two complementary isolation strategies maximized recovery of functionally relevant taxa. Diluted homogenates were first plated on non-selective, low-nutrient R2A agar to capture the broad

culturable bacterial community, including putative nitrogen-fixing and plant growth–promoting taxa, and incubated at 28°C for up to 15 days, with morphologically distinct colonies selected. In parallel, an Actinobacteria-focused enrichment used mild selective treatments and Actinobacteria-selective media (Sandrini et al. 2024; Bolyen et al. 2019) to recover slow-growing taxa.

Pure isolates were maintained on solid media and preserved as glycerol stocks at −80°C. Each isolate received a unique identifier encoding genotype, nitrogen treatment, and isolation strategy, and was taxonomically identified by 16S rRNA gene sequencing. Isolates were subsequently stored in the CREA – Research Centre for Viticulture and Enology microbial bank (https://www.revine-prima2020.org/vimed) as both lyophilized and glycerol stocks (40% v/v) at −80°C.

Root DNA isolation and metabarcoding analysis

DNA was extracted from ~50 mg of the same root samples used for bacterial isolation, following the manufacturer's protocol for the plant/fungi DNA isolation kit (Norgen Biotech Corp., Thorold, ON, Canada), using five biological replicates per treatment (randomly selected root fragments). DNA quantity and integrity were assessed by NanoDrop One spectrophotometry (Thermo Fisher Scientific, Waltham, MA, USA) and 1% agarose gel electrophoresis, with further quantification by Qubit 4 Fluorometer (Thermo Fisher Scientific) before sequencing. The V3–V4 region of the 16S rRNA gene was amplified with primers 319F (5′-CCTACGGGNGGCWGCAG-3′) and 806R (5′-GACTACHVGGGTATCTAATCC-3′). Raw amplicon reads were processed in QIIME 2 (Callahan et al. 2016): ASVs were inferred with DADA2 (Katoh et al. 2013) and placed on a phylogeny using the align-to-tree-mafft-fasttree pipeline (Price et al. 2010; Bokulich et al. 2018), and taxonomy was assigned with a Naïve Bayes classify-sklearn classifier trained on SILVA

(release 138, 99% OTUs) (Quast et al. 2013). Resulting artifacts and metadata were imported into R (R Core Team, 2020) and analysed with the microeco package (Liu et al. 2021).

Alpha diversity indices were calculated on data rarefied to 10,000 reads per sample (based on sequencing depth distribution), testing the effects of genotype, treatment and their interaction for each index. Since Shapiro–Wilk tests showed non-normal model residuals, indices were analysed by two-way aligned rank transform ANOVA (ART-ANOVA; Wobbrock et al. 2011), with genotype and treatment as fixed factors.

When the genotype × treatment interaction was non-significant, post-hoc comparisons were performed separately for genotype and treatment using Holm-adjusted pairwise tests (Lenth et al. 2026); estimated marginal means (± SE) on the original scale were used for data presentation.

Beta diversity was assessed on the rarefied dataset using Bray–Curtis dissimilarity (relative-abundance-based taxonomic composition) and weighted UniFrac distance (incorporating phylogenetic relationships and abundance) (Lozupone et al. 2007), with phylogenetic distances computed from the rooted tree generated during sequence processing. Principal coordinate analysis (PCoA) was applied to both matrices as an exploratory, unconstrained ordination to visualize community composition; no statistical inference was drawn directly from ordination plots.

Permutational multivariate analysis of variance (PERMANOVA) was performed with a full factorial model (genotype, treatment, NUE, and their interactions) separately for Bray–Curtis and weighted UniFrac distances (999 permutations; adonis2, by = "terms"). Homogeneity of multivariate dispersions was tested for all grouping factors (betadisper), and PERMANOVA results were interpreted in light of dispersion patterns, particularly where genotypes differed significantly.

Taxa driving sample separation were identified by ordinating phylum- or genus-level agglomerated abundance tables with principal component analysis (PCA). Putative ecological functions were inferred from taxonomy using FAPROTAX (Louca et al. 2016), which maps taxa to functional groups based on cultured representatives, applied to the SILVA-classified ASV table via the trans_func class of microeco (Liu et al. 2021) to compute per-sample functional relative abundances; as these annotations are taxonomy-inferred rather than measured, they were interpreted as functional potential rather than realised activity. All plots were generated in R with ggplot2 (Wickham et al. 2016).

Plant production traits statistics

Plant production traits (Supplementary Table 1) were summarized using principal component analysis (PCA) to reduce dimensionality and account for collinearity among correlated variables. PCA was performed on scaled production traits using the prcomp function in R, with centering and scaling applied to all variables. The interpretation of PC1 and PC2 was supported by trait loadings (Supplementary Table 2).

Principal component scores were subsequently used for statistical testing. Normality of model residuals was assessed using Shapiro–Wilk tests. When assumptions of normality were violated, differences in principal component scores were tested using aligned rank transform (ART) ANOVA, implemented with the ARTool package (Kay et al. 2025), including genotype, treatment, and their interaction as fixed effects. When significant main effects or interactions were detected, post hoc comparisons were performed using estimated marginal means with Holm-adjusted p-values. In the absence of significant interactions, marginal effects were evaluated; when interactions were present, simple effects were tested within each factor level.

237

Results

Ecophysiological responses to genotype and nitrogen treatment

Leaf gas exchange traits were largely unaffected by genotype or nitrogen supply. Pn and iACE showed no significant effect of genotype, nitrogen, or their interaction (all $p > 0.4$; Figure 2). iWUE showed a genotype-level trend ($F_{3,16} = 2.58$, $p = 0.090$) with no nitrogen or interaction effect ($p = 0.45$, 0.70): the low-nitrogen-affinity genotypes 305E40 and AM194 tended toward higher iWUE (27.4, 29.5 μmol CO_2 mol^{-1} H_2O) than high-nitrogen-affinity AM241 and 67/3 (21.4, 19.2), though Tukey HSD contrasts were non-significant (closest, 67/3 vs AM194, $p = 0.085$). Nitrogen supply did not significantly alter any parameter.

Composition of the culturable eggplant root microbiome

Across genotypes and nitrogen regimes, eggplant roots harbored a phylogenetically diverse culturable microbiome dominated by Firmicutes and Proteobacteria (Supplementary Table 3). The culturable fraction was largely *Bacillus* and related genera (*Fictibacillus, Mesobacillus, Metabacillus, Cytobacillus, Neobacillus*), consistently isolated across all conditions, indicating a stable association with the eggplant root niche; Proteobacterial taxa (*Agrobacterium, Rhizobium, Pseudomonas, Sphingobium, Sphingopyxis, Paracoccus, Lysobacter*) were recurrent but showed stronger genotype- and nitrogen-dependent patterns. Actinomycetes (*Streptomyces, Nocardia, Nocardioides, Microbacterium, Lentzea*) contributed substantially to culturable diversity, particularly under fertilized conditions (3N): none were isolated from 305E40 under either regime, and in 67/3 they were recovered exclusively under 3N, pointing to genotype-specific and, in 67/3, nitrogen-dependent recruitment of this group.

Alpha and β-diversity reveal genotype-dependent community structuring

Alpha diversity was assessed with complementary indices capturing richness (Observed), diversity/evenness (Shannon), rare-taxa-sensitive richness (Chao1), and evenness (Pielou).

Shannon diversity was significantly affected by genotype and treatment, with no significant interaction (ART-ANOVA; genotype: $F_{3,24} = 24.82$, $p < 0.001$; treatment: $F_{1,24} = 8.68$, $p = 0.007$; interaction: $F_{3,24} = 1.97$, $p = 0.15$), indicating treatment exerted a consistent effect across genotypes despite genotype-level diversity differences. Averaged across treatments, 305E40 and AM194 showed significantly higher Shannon diversity than AM241 and 67/3 (Holm-corrected; Figure 3a), with 67/3 lowest overall; averaged across genotypes, 3N exceeded 0N (mean ± SE: 5.36 ± 0.04 vs 5.24 ± 0.04; $p < 0.01$).

Observed richness was significantly affected by genotype ($F_{3,24} = 11.08$, $p < 0.001$; Figure 3b) but not treatment or their interaction ($p > 0.05$), indicating detectable taxon number was genotype-determined and stable across treatments. Post hoc tests showed 67/3 significantly lower than AM194 and 305E40 (Holm-adjusted $p < 0.05$), with AM241 intermediate and not significantly different from either extreme, and AM194/305E40 comparably highest — a clear genotype-driven richness gradient, lowest in 67/3 and highest in AM194/305E40.

Chao1 richness, in contrast, was significantly affected by genotype, treatment, and their interaction (genotype: $F_{3,24} = 9.64$, $p < 0.001$; treatment: $F_{1,24} = 4.87$, $p = 0.037$; interaction: $F_{3,24} = 3.91$, $p = 0.021$): post hoc tests showed a genotype-dependent treatment response, with Chao1 significantly increasing under 3N in 305E40 and AM241 but not in 67/3 or AM194.

Pielou's evenness likewise showed significant genotype, treatment, and interaction effects (genotype: $F_{3,24} = 14.08$, $p < 0.001$; treatment: $F_{1,24} = 21.50$, $p < 0.001$; interaction: $F_{3,24} = 4.30$, p

= 0.015), with treatment significantly altering evenness only in 305E40 (Holm-corrected p = 0.006).

PCoA on Bray–Curtis dissimilarity (Figure 4a) and weighted UniFrac distance (Figure 4b) showed clear treatment-based separation with additional genotype-driven clustering. PERMANOVA confirmed significant genotype, treatment, and interaction effects for both distances ($p = 0.001$ for all terms), with genotype explaining the most variance for weighted UniFrac ($R^2 = 0.465$; treatment $R^2 = 0.252$; interaction $R^2 = 0.156$) and a similar but weaker pattern for Bray–Curtis (genotype $R^2 = 0.260$, treatment $R^2 = 0.155$, interaction $R^2 = 0.215$). Dispersion did not differ among treatments, indicating treatment effects reflected compositional shifts rather than dispersion, whereas dispersion did differ among genotypes, suggesting genotype effects combine centroid and within-genotype variability differences.

Separate within-genotype PERMANOVAs confirmed nitrogen significantly affected community composition in all genotypes for both distances (adjusted $p < 0.05$), with effect magnitude varying by genotype (weighted UniFrac $R^2 = 0.70–0.82$; Bray–Curtis $R^2 = 0.47–0.53$); dispersion was again non-significant within genotypes, confirming true compositional shifts. All genotypes thus respond to nitrogen, but response strength is genotype-dependent.

Root microbiome composition and diversity across genotypes and nitrogen regimes

Root microbiome composition differed across genotypes and nitrogen regimes, mirroring the culturable isolates: Actinobacteriota were more abundant under 3N regardless of genotype, confirming the culture-based pattern; AM194 was consistently enriched in Acidobacteriota regardless of regime; 67/3 showed stable Firmicutes dominance under both regimes; and Proteobacteria dominated across treatments, most strongly in AM241 (Figure 5).

PCA on genus/phylum-level taxonomic profiles, performed to identify taxa driving sample separation, corroborated the PERMANOVA results, explaining 43.6% and 33.1% of variance along PC1 and PC2 (Figure 6). Samples clustered by genotype × treatment; 67/3 formed a clearly separated cluster along PC2 regardless of treatment, driven by higher loadings of *Bacillus* and *Pseudoxanthomonas*, whereas other genotypes associated more with *Lysobacter, Pseudoduganella, Massilia*, and the *Polyangium brachysporum* group.

This divergence of 67/3 was further resolved in the phylogenetic cladogram analysis (Figure 7), confirming its distinct composition, characterized mainly by *Firmicutes/Bacillus*; the Vicinamibacteria clade was specifically associated with AM194 and *Streptomyces* with AM241.

Differential abundance analysis (Supplementary Figure 1) further showed Actinobacteriota, Verrucomicrobiota, and Acidobacteriota significantly enriched under 3N and Bacteroidota under 0N, consistent with the culture-based nitrogen-dependent Actinomycetes recruitment noted above. Collectively, ordination and differential abundance analyses show host genotype shapes both taxonomic composition and phylogenetic structure; we next examined whether these communities also differ functionally.

Predicted functional profiles associated with genotype-specific microbiomes

Predicted functional profiling revealed genotype-dependent differences in functional potential (Figure 8): chemoheterotrophy (methylotrophy, nitrification, chitinolysis) and aerobic chemoheterotrophy (methanol oxidation, aerobic ammonia oxidation) dominated across all genotypes, reflecting the prevalence of heterotrophic taxa, while nitrogen-related functions (nitrate reduction, nitrogen respiration), fermentation, cellulolysis, and aromatic compound degradation varied among genotypes, mirroring compositional shifts. Genotype 67/3's functional profile

diverged most, with the lowest aerobic ammonia oxidation and nitrification, indicating its compositional divergence extends to function; AM194 and AM241 showed higher chitinolysis, 305E40 and AM241 had similar functional profiles, and AM194 had the highest nitrification/ammonia-oxidation potential. We next tested whether these compositional and functional differences related to plant production traits.

Linking root microbiome composition and plant performance

Production traits were summarized by PCA (Supplementary Figure 2): PC1 explained 75.0% of variance and PC2 an additional 9.95% (85.0% combined). PC1 loaded positively across fruit production, plant size, and biomass traits (≈0.26–0.33), reflecting overall productivity/vigor, and was retained as a synthetic host-performance descriptor; PC2, driven by leaf fresh weight (positive) and shoot dry matter content (negative), reflected biomass allocation and tissue water content rather than yield.

Since PC1 residuals were non-normal (Shapiro–Wilk $p = 0.0009$), an ART two-way ANOVA was used: PC1 was significantly affected by genotype ($F_{3,24} = 15.94$, $p < 0.001$) and nitrogen ($F_{1,24} = 65.49$, $p < 0.001$), with a significant interaction ($F_{3,24} = 3.15$, $p = 0.043$). Post hoc simple-effects tests (Holm-adjusted) showed nitrogen significantly increased PC1 only in AM241 ($p = 0.0296$), with no effect in other genotypes and no significant pairwise genotype comparisons within nitrogen levels.

Including PC1 as a continuous predictor in a PERMANOVA controlling for genotype and treatment showed genotype ($R^2 = 0.205$, $p = 0.001$) and treatment ($R^2 = 0.058$, $p = 0.001$) significantly explained community variation, but PC1 added no explanatory power ($R^2 = 0.024$, p

= 0.251) — microbiome structure was determined by genotype and nitrogen regime rather than productivity itself.

Discussion

The increasing attention on plant-associated microbiomes has shifted microbial diversity from a descriptive inventory of taxa to a functional component of plant adaptation and performance (Vandenkoornhuyse et al. 2015; Nerva et al. 2022a). This shift is particularly relevant for eggplant, whose root-associated and endophytic bacterial communities remain poorly characterized despite its agronomic relevance.

The eggplant root microbiome reflects selection at the interface of host genotype, nutrient availability and the surrounding microbial pool (Trivedi et al. 2020; Dastogeer et al. 2020), with genotype-specific metabolites and root architecture generating the niches governing colonization (Uribe-Acosta et al. 2025; Wagner et al. 2016; Sandrini et al. 2022b; Galindo-Castañeda et al. 2024). Since nitrogen shapes both eggplant productivity (Jilani et al. 2008; Mauceri et al. 2021) and root exudation/rhizosphere composition (Zhu et al. 2016), differences in nitrogen-use efficiency may reflect distinct belowground resource-acquisition and microbial-recruitment strategies. Combining 16S rRNA profiling with culture-dependent isolation resolved dominant and rarer lineages and yielded a culturable collection for future functional work, converging on one central finding: eggplant hosts genotype-specific bacterial assemblages, further modulated by nitrogen availability, rather than one uniform root microbiome.

Root-associated assemblages differed markedly among genotypes, indicating strong host genetic control over microbiome assembly, likely driven by genotype-specific root traits (exudation profiles, nutrient-uptake strategies, immune-mediated filtering), as seen in other crops and model

plants (Uribe-Acosta et al. 2025). Since all plants grew in the same substrate, genotype-dependent differences reflect differential filtering from a common microbial pool rather than inoculum variation, strengthening host genetic background as the primary driver of assembly here.

Proteobacteria dominance across all genotypes is consistent with previous eggplant studies, where this phylum is a major rhizosphere component across developmental stages (Zhang et al. 2024). Broad surveys of eggplant rhizosphere microbiota similarly identify Proteobacteria, Actinobacteriota, Acidobacteriota, Chloroflexi and Firmicutes as dominant, recurrent phyla, supporting a conserved core microbiome for this crop (Gong et al. 2024). Consistently, other eggplant rhizosphere analyses report strong dominance of Proteobacteria (particularly Gammaproteobacteria) and Firmicutes classes such as Clostridia and Bacilli, with comparatively less abundant Actinobacteria (Mandal et al. 2025). Together, these findings suggest that while a conserved core microbiome may exist at broader taxonomic levels, specific functional groups' abundance is highly context-dependent and shaped by nutrient-driven plant–microbe interactions. This strong genotype effect matches observations in other systems, including tomato, where plant identity is the primary factor structuring rhizosphere communities (Grunert et al 2019; Ahmad et al. 2024; Lanzavecchia et al. 2024; Han et al. 2025). Alpha diversity analysis supported this, identifying genotype as the primary determinant of microbial diversity across all indices. Similar genotype-driven effects occur in other crops, including wheat, where genetic background strongly structures microbial communities (Jacquiod et al. 2022). At the community level, beta diversity confirmed genotype as the primary driver of microbiome structure, explaining more variance than treatment or their interaction. Dispersion differences among genotypes further suggest host plants shape not just average composition but also the range of microbial configurations they support, potentially reflecting differences in ecological stability or filtering strength.

Nitrogen availability was a consistent, secondary environmental driver of assembly. In our system, Actinobacteriota occurrence strongly depended on nitrogen availability, detected predominantly under fertilized conditions, a pattern supported by both amplicon and culture-based data. Nitrogen inputs can increase microbial biomass and density by enhancing rhizosphere resource availability (Gieske et al. 2020), and promote plant growth and rhizodeposition, adding carbon substrates that support microbial proliferation (Zhu et al. 2016). Nitrogen effects on alpha diversity were correspondingly subtle, with higher diversity under fertilized conditions averaged across genotypes, suggesting genotype constrains overall assembly while nitrogen modulates diversity by enabling recruitment of additional taxa. This contrasts with tomato, where unfertilized conditions showed higher diversity and evenness (Grunert et al. 2019), highlighting the context-dependent nature of microbiome responses to nutrient inputs. The selective enrichment of Actinobacteria under fertilization warrants closer mechanistic scrutiny beyond general resource stimulation. Actinobacteria are broadly oligotrophic-to-copiotrophic intermediate strategists, particularly competitive where carbon and nitrogen are both available (Fierer et al. 2007; Hashim et al. 2026). Under nitrogen limitation, stoichiometric imbalances may disadvantage slower-growing, high-biomass-yield taxa like Actinobacteria relative to faster-cycling, more nitrogen-efficient groups, even with carbon available from root exudation (Cleveland et al. 2007). Nitrogen fertilization relieves this limitation, letting Actinobacteria compete and proliferate. Beyond stoichiometry, Actinobacteria also enrich as producers of secondary metabolites, including antibiotics and antifungal compounds (Barka et al., 2016; Viaene et al., 2016). Their increased abundance under fertilization could reshape competitive hierarchies within the root microbiome, suppressing susceptible taxa and contributing to the higher diversity and evenness under 3N — positioning Actinobacteria as active community structurers rather than passive responders. This

matches the broader literature on Actinobacteria as keystone taxa in soil and rhizosphere ecosystems (Mendes et al., 2011).

Within genotypes, nitrogen consistently altered community composition, but with varying magnitude — genotypes differ not in whether they respond to nitrogen, but in the extent of restructuring. Genotype 67/3's markedly low diversity and Firmicutes-dominated composition across both regimes represents this continuum's extreme, suggesting an unusually strong host filtering effect. While all genotypes showed nitrogen-dependent compositional shifts, 67/3 maintained a stable, Bacillus-enriched community regardless of treatment, pointing to host-driven rather than environmentally driven assembly. Several non-exclusive mechanisms could explain this pattern. First, genotype-specific differences in root exudate quantity and quality could favor Bacillus-related taxa. This is supported by recent rapeseed evidence, where kaempferol, a flavonoid root exudate, mediated genotype-specific Bacillaceae enrichment, and a kaempferol-deficient mutant failed to recruit this group entirely (Wang et al. 2026). If 67/3 similarly produces Bacillus-attracting exudates, this would explain its consistent dominance across nitrogen regimes. Second, roots deploy pattern-triggered immunity (PTI) and antimicrobial compounds that can selectively suppress some taxa while promoting others (Lebeis et al. 2015; Pascale et al. 2020). Differences in these defense pathways could explain the near-complete absence of Actinomycetes in 67/3 under both conditions, unlike any other genotype. If 67/3 maintains a constitutively active immune tone, this could suppress copiotrophic, slower-growing taxa like Actinobacteria, while Bacillus — which has well-characterized immune-evasion mechanisms — remains unaffected (Bulgarelli et al. 2013; Pieterse et al. 2014). Third, root architecture and anatomy can determine microbial access to root tissues, influencing which taxa colonize the endosphere versus remaining confined to the rhizosphere (Galindo-Castañeda et al. 2024). Genotype-specific differences in root

morphology, lateral root density, root hair abundance, or cell wall composition could affect colonizing bacteria's spatial distribution and diversity, contributing to 67/3's lower richness and evenness. Whether these mechanisms act independently or synergistically remains untested; future studies combining exudate profiling, immune-gene transcriptomics, and root architectural characterization across genotypes would offer mechanistic insight.

The ecological consequences of a constrained microbiome are not straightforward. On one hand, low diversity and single-taxon dominance could be a functional limitation, reducing the range of microbial services available to the plant. On the other hand, a tightly filtered, Bacillus-dominated community may sustain key plant-beneficial functions through alternative pathways. Several Bacillus species like *B. megaterium, B. cereus, B. pumilus, B. subtilis* function as diazotrophs, fixing atmospheric nitrogen (Saxena et al. 2020). A Bacillus strain isolated from an N-use-efficient rapeseed genotype's rhizosphere was also shown to enhance root biomass and nitrogen uptake in an N-use-inefficient genotype (Wang et al. 2026). This raises the possibility that 67/3's Bacillus-dominated microbiome sustains nitrogen acquisition through direct plant-growth-promoting activity rather than community-level cycling a functionally distinct but potentially effective strategy. Whether the Bacillus strains isolated from 67/3 exhibit measurable nitrogenase activity remains untested and would be a valuable direction for future functional work.

Among less abundant but noteworthy taxa, Vicinamibacteria were specifically associated with AM194 regardless of nitrogen regime, while *Polyangium brachysporum* group members were enriched in other genotypes. Vicinamibacteriales are reported as dominant in acidic soils and peatlands, with genomic evidence suggesting roles in phosphorus solubilization and carbon metabolism via bacterial microcompartments (Dedysh et al. 2022; Wu et al. 2021). Their enrichment in AM194 may thus reflect genotype-driven recruitment of phosphorus-cycling taxa,

potentially contributing to this genotype's nutrient-acquisition strategy. However, Vicinamibacteria's functional role in crop rhizospheres remains poorly characterized, and their consistent association with AM194 warrants further genome-resolved metagenomics investigation.

These compositional differences were paralleled by shifts in predicted functional potential. Functional profiles were derived from taxonomy-based predictive inference rather than direct metagenomics or metatranscriptomics, and should be interpreted as functional potential rather than confirmed activity. Functions related to chemoheterotrophy and aerobic chemoheterotrophy were dominant across all genotypes, consistent with the prevalence of heterotrophic taxa. However, nitrogen-related functions including nitrification and aerobic ammonia oxidation varied among genotypes, indicating differing predicted capacity for nitrogen transformations. Microbial oxidation of ammonia to nitrite, and its conversion to nitrate, are key nitrogen-cycling steps directly influencing plant nutrient availability (Grunert et al. 2019). Reduced representation of these functions in 67/3 matches its low Actinobacteriota abundance and suggests limited community-level nitrogen-cycling potential, whereas their enrichment elsewhere reflects a more functionally versatile microbiome. Chitinolysis and organic-matter-degradation functions were additionally enriched in AM194 and AM241, suggesting increased nutrient-turnover capacity. Chitin degradation contributes to carbon and nitrogen recycling and is mediated by complex microbial consortia (Wieczorek et al. 2019); enriched chitinolytic potential in these genotypes may reflect a more dynamic microbial community sustaining rhizosphere nutrient cycling.

Despite these functional differences, no direct association between overall microbiome composition and plant productivity was detected at the community level. PERMANOVA including productivity (PC1) as a continuous variable showed microbiome variation was primarily explained

by genotype and nitrogen regime, with no additional contribution from the productivity gradient. This suggests microbiome assembly and plant performance are parallel responses to host background and environment, rather than a direct microbiome-driven effect on productivity. Nevertheless, genotype-specific patterns suggest a potential indirect link between microbiome functional potential and host responsiveness. Only AM241 showed a significant productivity increase under fertilization, and was characterized by higher alpha diversity, Proteobacteria/Streptomyces enrichment, and broader predicted functional potential. This matches rapeseed findings, where N-use-efficient genotypes recruited more diverse communities and specific Bacillus strains actively promoted nitrogen acquisition (Wang et al. 2026), suggesting microbiome diversity and functional breadth may help the plant–microbiome system respond to nutrient changes. Causality cannot be inferred from the present data, and these patterns should be interpreted as hypothesis-generating observations. Beyond productivity, plant gas exchange provided a complementary readout of host performance. Under our conditions, leaf-level gas exchange was stable across nitrogen regimes and carbon assimilation did not differ among genotypes, indicating the contrasting root microbiomes above were not mirrored by large photosynthetic differences at sampling. The only structured pattern was a non-significant trend toward higher intrinsic water-use efficiency in the two low-nitrogen-affinity genotypes (305E40, AM194), reflecting lower stomatal conductance relative to assimilation. Though this separation didn't reach significance, its independence from nitrogen supply fits a constitutive, genotype-determined water-use strategy rather than a plastic N response — echoing the genotype-driven structuring seen in the root microbiome. Larger replication would confirm whether low-N-affinity genotypes are intrinsically more water-use efficient and whether this covaries with their distinct microbial recruitment.

Combining amplicon-based profiling with culture-dependent isolation provided a comprehensive characterization of the eggplant root microbiome. The two approaches converged on the dominant taxa (Bacillus, Actinomycetes), supporting the ecological relevance of the isolate collection, while amplicon sequencing additionally captured taxa poorly recovered by culturing, such as Acidobacteriota (Rappé et al. 2003) and Vicinamibacteria, whose functional roles remain a priority for future metagenomic work. Overall, host genotype shaped both microbiome composition and predicted functional potential, with nitrogen availability acting as a consistent secondary modulator, indicating that eggplant genotypes differ in the microbial taxa they recruit and in their degree of microbiome plasticity. Building on the resulting bacterial isolate collection, future work should link microbial identity to function through DMCs and controlled inoculation experiments, testing whether genotype-associated consortia contribute to nitrogen-use efficiency and plant performance, ultimately supporting tailored DMC strategies for sustainable crop management.

Ethics declarations

Ethics approval and consent to participate

Not applicable.

Consent for publication

Not applicable.

Competing interest

The authors declare that they have no known competing interests.

Funding

This work has been supported by AGER 3 Project – Micro4Life (Grant n◦ 2022–2903), by the Agritech National Research Center and received funding from the European Union Next-Generation EU (PIANO NAZIONALE DI RIPRESA E RESILIENZA (PNRR)—MISSIONE 4 COMPONENTE 2, INVESTIMENTO 1.4—D.D. 1032 17/06/2022, CN00000022) and by CIRCOVINO project (founded by the Italian Ministry of Environment and Energy Security, EC-DEC n. 86 of 07 September 2023). This manuscript reflects only the authors' views and opinions, neither the European Union nor the European Commission can be considered responsible for them.

Data availability

The raw 16S rRNA gene amplicon sequencing reads generated in this study have been deposited in the NCBI Sequence Read Archive (SRA) under BioProject accession number PRJNA1516020. Bacterial isolates obtained in this study are preserved in the CREA – Research Centre for Viticulture and Enology microbial culture collection (https://www.revine-prima2020.org/vimed) and are available from the corresponding authors upon request.

References

Ahmad W, Coffman L, Ray RL, Balan V, Weerasooriya A, Khan AL. Microbiome diversity and variations in industrial hemp genotypes. Scientific Reports 2024;14(1):29560. https://doi.org/10.1038/s41598-024-79192-7.

Barchi L, Rabanus-Wallace MT, Prohens J, Toppino L, Padmarasu S, Portis E, Rotino GL, Stein N, Lanteri S, Giuliano G. Improved genome assembly and pan-genome provide key insights into eggplant domestication and breeding. The Plant Journal 2021;107(2):579–96. https://doi.org/10.1111/tpj.15313.

Barka EA, Vatsa P, Sanchez L, Gaveau-Vaillant N, Jacquard C, Klenk HP, Clément C, Ouhdouch Y, van Wezel GP. Taxonomy, Physiology, and Natural Products of Actinobacteria. Microbiology and Molecular Biology Reviews 2016;80(1):1–43. https://doi.org/10.1128/mmbr.00019-15.

Baudoin E, Benizri E, Guckert A. Impact of artificial root exudates on the bacterial community structure in bulk soil and maize rhizosphere. Soil Biology and Biochemistry 2003;35(9):1183–92. https://doi.org/10.1016/S0038-0717(03)00179-2.

Bokulich NA, Kaehler BD, Rideout JR, Dillon M, Bolyen E, Knight R, Huttley GA, Caporaso JG. Optimizing taxonomic classification of marker-gene amplicon sequences with QIIME 2's q2-feature-classifier plugin. Microbiome 2018;6(1):90. https://doi.org/10.1186/s40168-018-0470-z.

Bolyen E, Rideout JR, Dillon MR, Bokulich NA, Abnet CC, Al-Ghalith GA, et al. Reproducible, interactive, scalable and extensible microbiome data science using QIIME 2. Nature Biotechnology 2019;37(8):852–7. https://doi.org/10.1038/s41587-019-0209-9.

Bulgarelli D, Schlaeppi K, Spaepen S, Ver Loren van Themaat E, Schulze-Lefert P. Structure and Functions of the Bacterial Microbiota of Plants. Annual Review of Plant Biology 2013;64:807–38. https://doi.org/10.1146/annurev-arplant-050312-120106.

Callahan BJ, McMurdie PJ, Rosen MJ, Han AW, Johnson AJA, Holmes SP. DADA2: High-resolution sample inference from Illumina amplicon data. Nature Methods 2016;13(7):581–3. https://doi.org/10.1038/nmeth.3869.

Cleveland CC, Liptzin D. C:N:P stoichiometry in soil: is there a "Redfield ratio" for the microbial biomass? Biogeochemistry 2007;85(3):235–52. https://doi.org/10.1007/s10533-007-9132-0.

Dastogeer KMG, Tumpa FH, Sultana A, Akter MA, Chakraborty A. Plant microbiome – an account of the factors that shape community composition and diversity. Current Plant Biology 2020;23:100161. https://doi.org/10.1016/j.cpb.2020.100161.

Dedysh SN, Ivanova AA, Begmatov ShA, Beletsky AV, Rakitin AL, Mardanov AV, Philippov DA, Ravin NV. Acidobacteria in Fens: Phylogenetic Diversity and Genome Analysis of the Key Representatives. Microbiology 2022;91(6):662–70. https://doi.org/10.1134/S0026261722601440.

Fierer N, Bradford MA, Jackson RB. Toward an ecological classification of soil bacteria. Ecology 2007;88(6):1354–64. https://doi.org/10.1890/05-1839.

Flexas J, Gulías J, Jonasson S, Medrano H, Mus M. Seasonal patterns and control of gas exchange in local populations of the Mediterranean evergreen shrub Pistacia lentiscus L. Acta Oecologica 2001;22(1):33–43. https://doi.org/10.1016/S1146-609X(00)01099-7.

Gaccione L, Toppino L, Bolger M, Schmidt M, Tassone MR, Sulli M, Idahl E, Alonso D, Aprea G, Ferrante P, Lefebvre V, Boyaci HF, Schafleitner R, Gattolin S, Finkers R, Brouwer M, Bovy A, Prohens J, Portis E, Lanteri S, Rotino GL, Giuliano G, Usadel B, Barchi L. Graph-based pangenomes and pan-phenome provide a cornerstone for eggplant biology and breeding. Nature Communications 2025;16(1):9919. https://doi.org/10.1038/s41467-025-64866-1.

Galindo-Castañeda T, Hartmann M, Lynch JP. Location: root architecture structures rhizosphere microbial associations. Journal of Experimental Botany 2024;75(2):594–604. https://doi.org/10.1093/jxb/erad421.

Gieske MF, Kinkel LL. Long-term nitrogen addition in maize monocultures reduces in vitro inhibition of actinomycete standards by soil-borne actinomycetes. FEMS Microbiology Ecology 2020;96(11):fiaa181. https://doi.org/10.1093/femsec/fiaa181.

Gong C, Wang Z, Li Z, Sun B, Luo W, Luo S, Chen S, Mai P, Li Z, Li Y, Wang Y, Li T. A QTL of eggplant shapes the rhizosphere bacterial community, co-responsible for resistance to bacterial wilt. Horticulture Research 2024;11(2):uhad272. https://doi.org/10.1093/hr/uhad272.

Gralka M, Szabo R, Stocker R, Cordero OX. Trophic Interactions and the Drivers of Microbial Community Assembly. Current Biology 2020;30(19):R1176–88. https://doi.org/10.1016/j.cub.2020.08.007.

Grunert O, Robles-Aguilar AA, Hernandez-Sanabria E, Schrey SD, Reheul D, Van Labeke MC, Vlaeminck SE, Vandekerckhove TGL, Mysara M, Monsieurs P, Temperton VM, Boon N, Jablonowski ND. Tomato plants rather than fertilizers drive microbial community structure in horticultural growing media. Scientific Reports 2019;9(1):9561. https://doi.org/10.1038/s41598-019-45290-0.

Han X, Zhang X, Su M, Yang S, Feng S, Tian T, Chen N, Zhao G, Huang L, Wang G. Genotype-specific rhizosphere microbiome assembly and its impact on soybean (Glycine max (L.) Merr.) yield traits. Frontiers in Sustainable Food Systems 2025;9:1518597. https://doi.org/10.3389/fsufs.2025.1518597.

Hao C, Dungait JAJ, Wei X, Ge T, Kuzyakov Y, Cui Z, Tian J, Zhang F. Maize root exudate composition alters rhizosphere bacterial community to control hotspots of hydrolase activity in response to nitrogen supply. Soil Biology and Biochemistry 2022;170:108717. https://doi.org/10.1016/j.soilbio.2022.108717.

Hashim HS, Zayan MM, Mohamed AA, Abd El-Rahman Abulila HI. Actinomycetes in the spotlight: biodiversity and their role in bioremediation. World Journal of Microbiology and Biotechnology 2026;42(2):44. https://doi.org/10.1007/s11274-025-04610-5.

Jacquiod S, Raynaud T, Pimet E, Ducourtieux C, Casieri L, Wipf D, Blouin M. Wheat Rhizosphere Microbiota Respond to Changes in Plant Genotype, Chemical Inputs, and Plant Phenotypic Plasticity. Frontiers in Ecology and Evolution 2022;10:903008. https://doi.org/10.3389/fevo.2022.903008.

Jilani MS, Afzal MF, Waseem K. Effect of different nitrogen levels on growth and yield of brinjal (Solanum melongena L.). Journal of Agricultural Research 2008;46(3):245–51. https://doi.org/10.58475/7mp0wc87.

Katoh K, Standley DM. MAFFT Multiple Sequence Alignment Software Version 7: Improvements in Performance and Usability. Molecular Biology and Evolution 2013;30(4):772–80. https://doi.org/10.1093/molbev/mst010.

Kay M, Elkin L, Higgins JJ, Wobbrock JO. mjskay/ARTool: ARTool 0.11.2 (v0.11.2). Zenodo, 2025. https://doi.org/10.5281/zenodo.15192343.

Kiran KR, Kaniyassery A, Murali TS, Muthusamy A. Fungal endophytes contribute to enhancing salinity stress tolerance in eggplant (Solanum melongena L.). Vegetos 2025. https://doi.org/10.1007/s42535-025-01289-9.

Koch H, Clavel T, Mayr C, Coltman BL, Schloter M, Vorholt JA, et al. From “synthetic” to defined microbial communities for clearer terminology. Nature Communications 2026;17(1):5283. https://doi.org/10.1038/s41467-026-74251-1.

Lanzavecchia G, Frascarelli G, Rocchetti L, Bellucci E, Bitocchi E, Di Vittori V, Sillo F, Ferraris I, Carta G, Delledonne M, Nanni L, Papa R. Genotype Combinations Drive Variability in the Microbiome Configuration of the Rhizosphere of Maize/Bean Intercropping System. International Journal of Molecular Sciences 2024;25(2):1288. https://doi.org/10.3390/ijms25021288.

Lebeis SL, Paredes SH, Lundberg DS, Breakfield N, Gehring J, McDonald M, Malfatti S, Glavina del Rio T, Jones CD, Tringe SG, Dangl JL. Salicylic acid modulates colonization of the root microbiome by specific bacterial taxa. Science 2015;349(6250):860–4. https://doi.org/10.1126/science.aaa8764.

Lenth RV, Piaskowski J. emmeans: Estimated Marginal Means, aka Least-Squares Means. R package version 2.0.5, 2026. https://rvlenth.github.io/emmeans/ (19 Aug. 2026, date last accessed).

Liu C, Cui Y, Li X, Yao M. microeco: an R package for data mining in microbial community ecology. FEMS Microbiology Ecology 2021;97(2):fiaa255. https://doi.org/10.1093/femsec/fiaa255.

Louca S, Parfrey LW, Doebeli M. Decoupling function and taxonomy in the global ocean microbiome. Science 2016;353(6305):1272–7. https://doi.org/10.1126/science.aaf4507.

Lozupone CA, Hamady M, Kelley ST, Knight R. Quantitative and Qualitative β Diversity Measures Lead to Different Insights into Factors That Structure Microbial Communities. Applied and Environmental Microbiology 2007;73(5):1576–85. https://doi.org/10.1128/AEM.01996-06.

Mandal M, Ghosh B, Mandal S. Comparison of the rhizospheric soil bacteriomes of Oryza sativa and Solanum melongena crop cultivars reveals key genes and pathways involved in biosynthesis of ectoine, lysine, and catechol meta-cleavage. Functional & Integrative Genomics 2025;25(1):20. https://doi.org/10.1007/s10142-025-01536-x.

Mauceri A, Bassolino L, Lupini A, Badeck F, Rizza F, Schiavi M, Toppino L, Abenavoli MR, Rotino GL, Sunseri F. Genetic variation in eggplant for Nitrogen Use Efficiency under contrasting NO3– supply. Journal of Integrative Plant Biology 2020;62(4):487–508. https://doi.org/10.1111/jipb.12823.

Mauceri A, Abenavoli MR, Toppino L, Panda S, Mercati F, Aci MM, Aharoni A, Sunseri F, Rotino GL, Lupini A. Transcriptomics reveal new insights into molecular regulation of nitrogen use efficiency in Solanum melongena. Journal of Experimental Botany 2021;72(12):4237–53. https://doi.org/10.1093/jxb/erab121.

Mendes R, Kruijt M, de Bruijn I, Dekkers E, van der Voort M, Schneider JHM, Piceno YM, DeSantis TZ, Andersen GL, Bakker PAHM, Raaijmakers JM. Deciphering the Rhizosphere Microbiome for Disease-Suppressive Bacteria. Science 2011;332(6033):1097–100. https://doi.org/10.1126/science.1203980.

Nerva L, Sandrini M, Moffa L, Velasco R, Balestrini R, Chitarra W. Breeding toward improved ecological plant–microbiome interactions. Trends in Plant Science 2022a;27(11):1134–43. https://doi.org/10.1016/j.tplants.2022.06.004.

Nerva L, Garcia JF, Favaretto F, Giudice G, Moffa L, Sandrini M, Cantu D, Zanzotto A, Gardiman M, Velasco R, Gambino G, Chitarra W. The hidden world within plants: metatranscriptomics unveils the complexity of wood microbiomes. Journal of Experimental Botany 2022b;73(8):2682–97. https://doi.org/10.1093/jxb/erac032.

Pascale A, Proietti S, Pantelides IS, Stringlis IA. Modulation of the Root Microbiome by Plant Molecules: The Basis for Targeted Disease Suppression and Plant Growth Promotion. Frontiers in Plant Science 2020;10:1741. https://doi.org/10.3389/fpls.2019.01741.

Pieterse CMJ, Zamioudis C, Berendsen RL, Weller DM, Van Wees SCM, Bakker PAHM. Induced Systemic Resistance by Beneficial Microbes. Annual Review of Phytopathology 2014;52:347–75. https://doi.org/10.1146/annurev-phyto-082712-102340.

Price MN, Dehal PS, Arkin AP. FastTree 2 – Approximately Maximum-Likelihood Trees for Large Alignments. PLOS ONE 2010;5(3):e9490. https://doi.org/10.1371/journal.pone.0009490.

Quast C, Pruesse E, Yilmaz P, Gerken J, Schweer T, Yarza P, Peplies J, Glöckner FO. The SILVA ribosomal RNA gene database project: improved data processing and web-based tools. Nucleic Acids Research 2013;41(D1):D590–6. https://doi.org/10.1093/nar/gks1219.

R Core Team. R: A Language and Environment for Statistical Computing. Vienna: R Foundation for Statistical Computing, 2020. https://www.R-project.org/.

Rappé MS, Giovannoni SJ. The Uncultured Microbial Majority. Annual Review of Microbiology 2003;57:369–94. https://doi.org/10.1146/annurev.micro.57.030502.090759.

Sandrini M, Nerva L, Sillo F, Balestrini R, Chitarra W, Zampieri E. Abiotic Stress and Belowground Microbiome: The Potential of Omics Approaches. International Journal of Molecular Sciences 2022a;23(3):1091. https://doi.org/10.3390/ijms23031091.

Sandrini M, Moffa L, Velasco R, Balestrini R, Chitarra W, Nerva L. Microbe-assisted crop improvement: a sustainable weapon to restore holobiont functionality and resilience. Horticulture Research 2022b;9:uhac160. https://doi.org/10.1093/hr/uhac160.

Sandrini M, Chitarra W, Pagliarani C, Moffa L, Petrozziello M, Colla P, Velasco R, Balestrini R, Nerva L. Microbial consortia inoculants differently shape ecophysiological and systemic defence responses of field-grown grapevine cuttings. Plant Stress 2024;14:100686. https://doi.org/10.1016/j.stress.2024.100686.

Saxena AK, Kumar M, Chakdar H, Anuroopa N, Bagyaraj DJ. Bacillus species in soil as a natural resource for plant health and nutrition. Journal of Applied Microbiology 2020;128(6):1583–94. https://doi.org/10.1111/jam.14506.

Singh SK, Wu X, Shao C, Zhang H. Microbial enhancement of plant nutrient acquisition. Stress Biology 2022;2(1):3. https://doi.org/10.1007/s44154-021-00027-w.

Toppino L, Barchi L, Mercati F, Acciarri N, Perrone D, Martina M, Gattolin S, Sala T, Fadda S, Mauceri A, Ciriaci T, Carimi F, Portis E, Sunseri F, Lanteri S, Rotino GL. A New Intra-Specific and High-Resolution Genetic Map of Eggplant Based on a RIL Population, and Location of QTLs Related to Plant Anthocyanin Pigmentation and Seed Vigour. Genes 2020;11(7):745. https://doi.org/10.3390/genes11070745.

Trivedi P, Leach JE, Tringe SG, Sa T, Singh BK. Plant–microbiome interactions: from community assembly to plant health. Nature Reviews Microbiology 2020;18(11):607–21. https://doi.org/10.1038/s41579-020-0412-1.

Uribe-Acosta M, Pascale A, Zhou J, Stringlis IA, Pieterse CMJ. Roots: metabolic architects of beneficial microbiome assembly. Plant Physiology 2025;199(1):kiaf349. https://doi.org/10.1093/plphys/kiaf349.

Vandenkoornhuyse P, Quaiser A, Duhamel M, Le Van A, Dufresne A. The importance of the microbiome of the plant holobiont. New Phytologist 2015;206(4):1196–206. https://doi.org/10.1111/nph.13312.

Viaene J, Van Lancker J, Vandecasteele B, Willekens K, Bijttebier J, Ruysschaert G, De Neve S, Reubens B. Opportunities and barriers to on-farm composting and compost application: A case study from northwestern Europe. Waste Management 2016;48:181–92. https://doi.org/10.1016/j.wasman.2015.09.021.

Wagner MR, Lundberg DS, del Rio TG, Tringe SG, Dangl JL, Mitchell-Olds T. Host genotype and age shape the leaf and root microbiomes of a wild perennial plant. Nature Communications 2016;7(1):12151. https://doi.org/10.1038/ncomms12151.

Wang Y, Zhao D, Li Z, Yang Y, Peng Z, Meng C, Ma S, Xu K, Li Y, Ding G, Zheng Y, Zhang CS. Kaempferol drives genotype-specific microbiota Bacillaceae to enhance nitrogen acquisition in rapeseed. Journal of Advanced Research 2026;82:127–39. https://doi.org/10.1016/j.jare.2025.07.018.

Wickham H. ggplot2: Elegant Graphics for Data Analysis. Use R! Cham: Springer International Publishing, 2016. https://doi.org/10.1007/978-3-319-24277-4.

Wieczorek AS, Schmidt O, Chatzinotas A, von Bergen M, Gorissen A, Kolb S. Ecological Functions of Agricultural Soil Bacteria and Microeukaryotes in Chitin Degradation: A Case Study. Frontiers in Microbiology 2019;10:1293. https://doi.org/10.3389/fmicb.2019.01293.

Wobbrock JO, Findlater L, Gergle D, Higgins JJ. The aligned rank transform for nonparametric factorial analyses using only anova procedures. In: Proceedings of the SIGCHI Conference on Human Factors in Computing Systems (CHI '11). New York, NY, USA: ACM, 2011:143–6. https://doi.org/10.1145/1978942.1978963.

Wu X, Peng J, Liu P, Bei Q, Rensing C, Li Y, Yuan H, Liesack W, Zhang F, Cui Z. Metagenomic insights into nitrogen and phosphorus cycling at the soil aggregate scale driven by organic material amendments. Science of The Total Environment 2021;785:147329. https://doi.org/10.1016/j.scitotenv.2021.147329.

Yu RP, Yang H, Xing Y, Zhang WP, Lambers H, Li L. Belowground processes and sustainability in agroecosystems with intercropping. Plant and Soil 2022;476(1):263–88. https://doi.org/10.1007/s11104-022-05487-1.

Zhang J, Liu W, Bu J, Lin Y, Bai Y. Host genetics regulate the plant microbiome. Current Opinion in Microbiology 2023;72:102268. https://doi.org/10.1016/j.mib.2023.102268.

Zhang Y, Gan G, Li Y, Li W, Jiang Y, Wang P, Hu J, Wang N, Quan X, Liu J, Raza W, Xu Y, Hohmann P, Jousset A, Wang Y, Shen Q, Jiang G, Wei Z. Exploring the temporal dynamics of a disease suppressive rhizo-microbiome in eggplants. iScience 2024;27(7):110319. https://doi.org/10.1016/j.isci.2024.110319.

Zhu S, Vivanco JM, Manter DK. Nitrogen fertilizer rate affects root exudation, the rhizosphere microbiome and nitrogen-use-efficiency of maize. Applied Soil Ecology 2016;107:324–33. https://doi.org/10.1016/j.apsoil.2016.07.009.

Figure titles and legends:

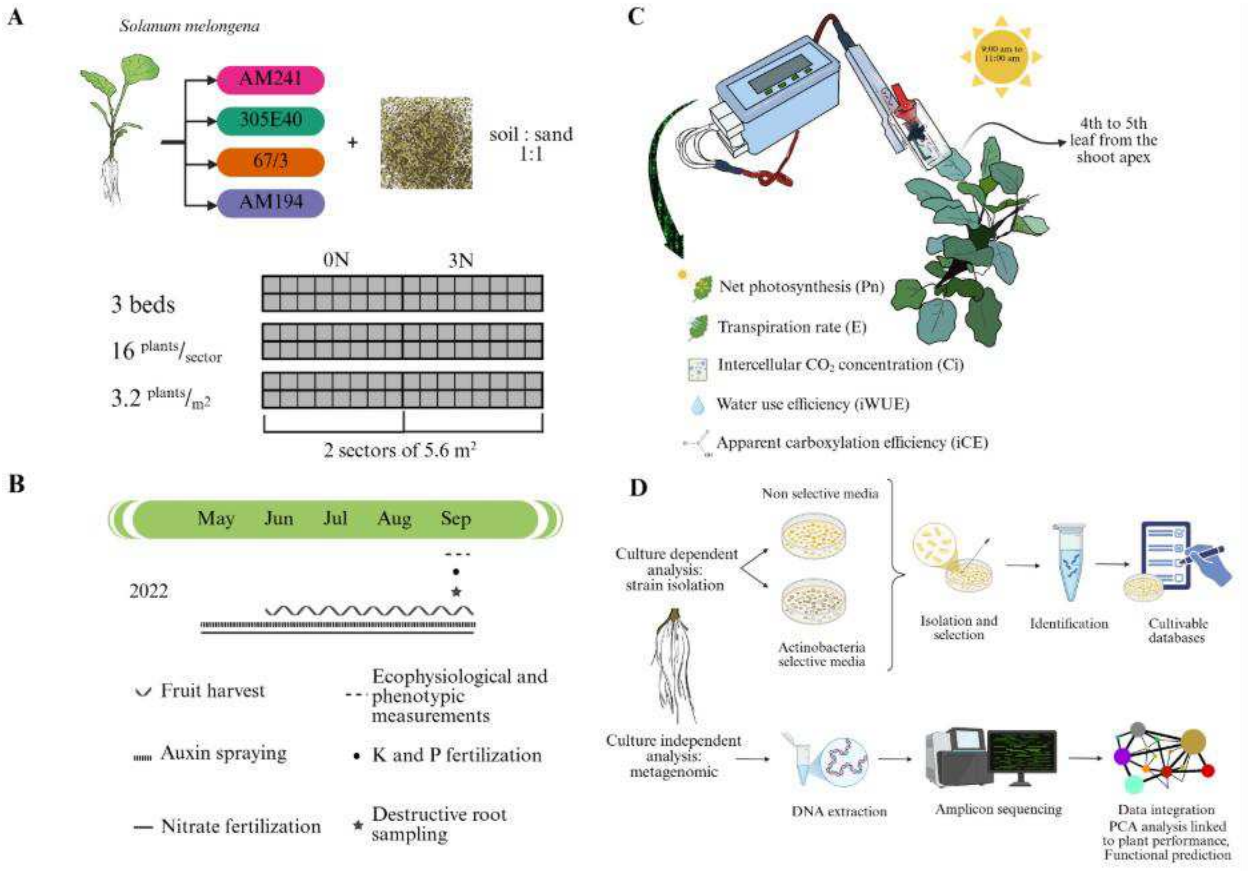


Figure 1 - Experimental design and analytical workflow. (A) Four eggplant (*Solanum melongena*) genotypes: AM241, 305E40, 67/3 and AM194 were grown in a 1:1 soil:sand substrate across three beds, each divided into two sectors of 5.6 m² (16 plants per sector; 3.2 plants m^{-2}), under two nitrogen regimes (0N, unfertilised; 3N, nitrate-fertilised). (B) Timeline of the 2022 growing season (May–September) showing management and sampling events: nitrate fertilisation (solid line), auxin spraying (hatched line), potassium and phosphorus fertilisation (dots), fruit harvest, ecophysiological and phenotypic measurements (dashed line), and destructive root sampling (star). (C) Leaf gas exchange was measured on the 4th–5th leaf from the shoot apex between 09:00 and 11:00 using a portable open-flow gas-exchange system, recording net photosynthesis (P_n), transpiration (E) and intercellular CO_2 concentration (C_i), from which intrinsic water-use efficiency and apparent carboxylation efficiency were derived. (D) Root-associated bacteria were characterised through a dual approach: culture-dependent isolation on non-selective and Actinobacteria-selective media, followed by strain isolation, identification and deposition in a cultivable-strain database; and culture-independent amplicon sequencing, comprising DNA extraction, 16S rRNA gene sequencing, and data integration including PCA linked to plant performance and functional prediction.

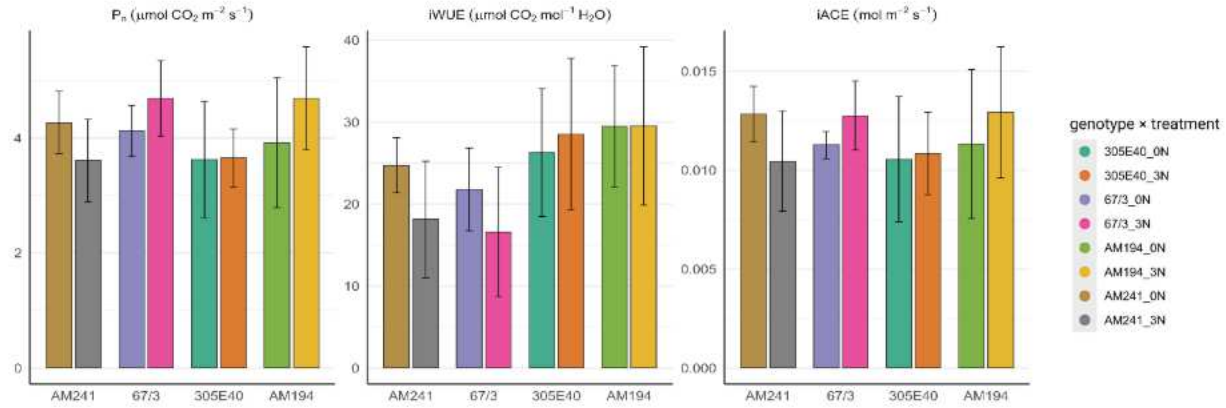


Figure 2 - **Leaf gas-exchange traits of four eggplant genotypes under two nitrogen regimes.** Net photosynthesis (P_n; μmol CO_2 m^{-2} s^{-1}), intrinsic water-use efficiency (iWUE = P_n/g_s; μmol CO_2 mol^{-1} H_2O) and intrinsic carboxylation efficiency (iACE = P_n/c_i; mol m^{-2} s^{-1}) measured in genotypes AM241, 67/3, 305E40 and AM194 grown under nitrogen limitation (0N) and nitrogen fertilization (3N). Bars represent the mean of three biological replicates (n = 3) and error bars denote ± standard deviation; fill colour indicates each genotype × nitrogen combination. Traits were compared by two-way ANOVA (genotype × nitrogen) followed by Tukey's HSD. The absence of letter groupings reflects the lack of significant pairwise differences (Tukey's HSD, $P > 0.05$).

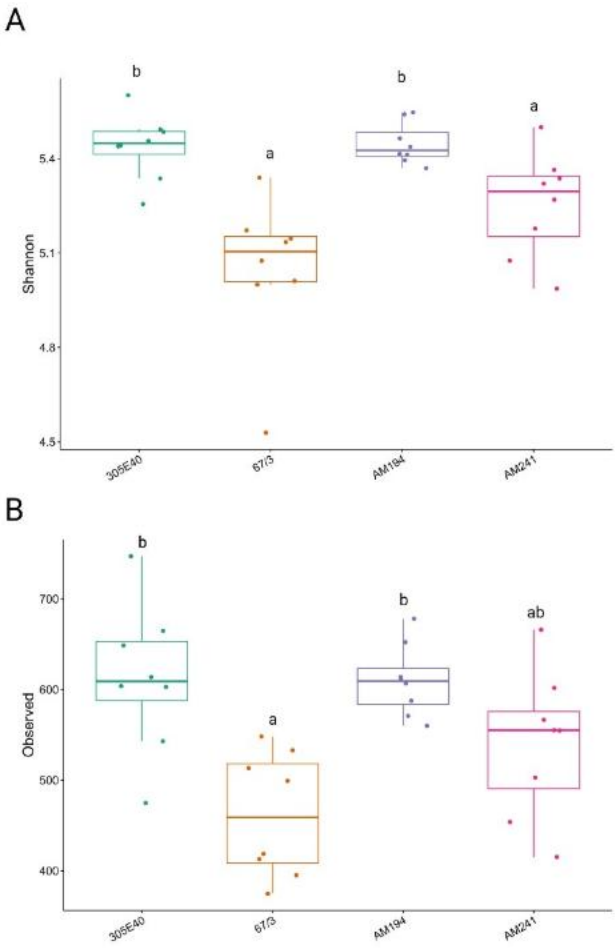


Figure 3 - Alpha diversity indices across genotypes (A–B). Shannon diversity index (A) and observed richness (B) were calculated on rarefied data. Alpha diversity was analysed using two-way aligned rank transform ANOVA (ART-ANOVA) with genotype and treatment as fixed factors. As no significant genotype × treatment interaction was detected, post hoc comparisons were performed for genotype using Holm-adjusted pairwise tests. Different letters indicate significant differences among genotypes ($p < 0.05$). Data are presented as estimated marginal means (± SE) on the original scale, and points represent individual samples.

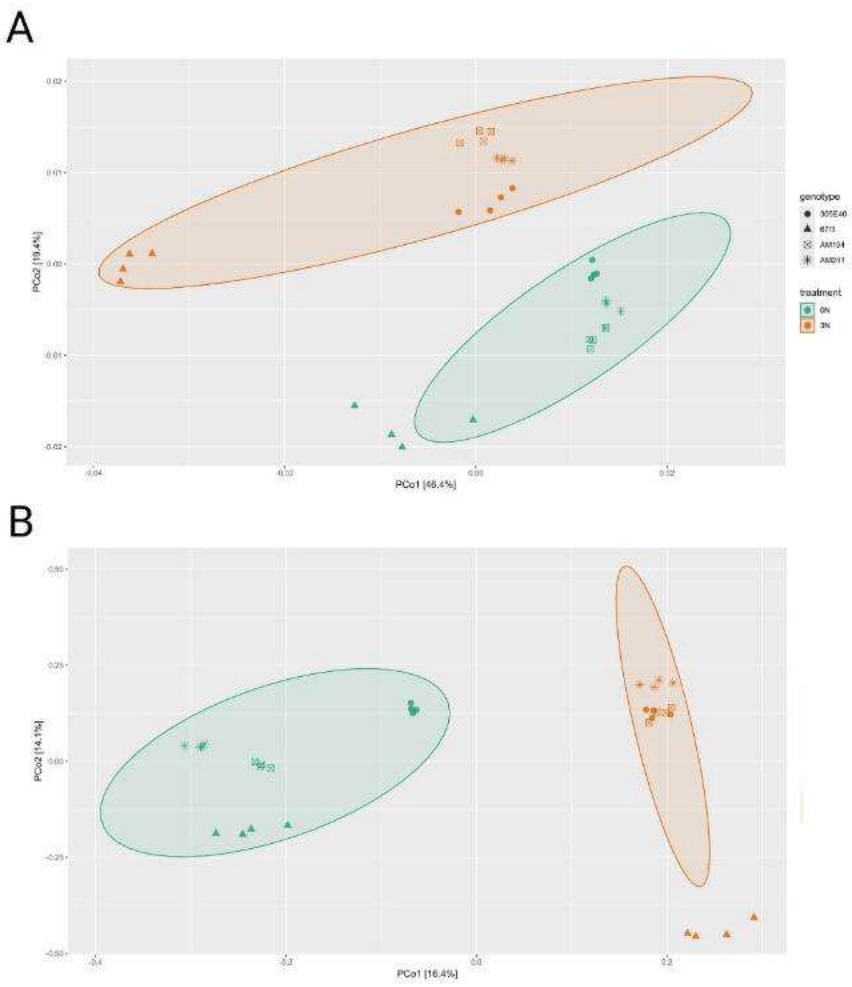


Figure 4. Principal coordinate analysis (PCoA) of microbial community composition based on Bray–Curtis dissimilarity (A) and weighted UniFrac distance (B). Samples are colored by treatment and shaped by genotype. Ellipses represent 95% confidence intervals. Statistical significance of group differences was assessed using PERMANOVA.

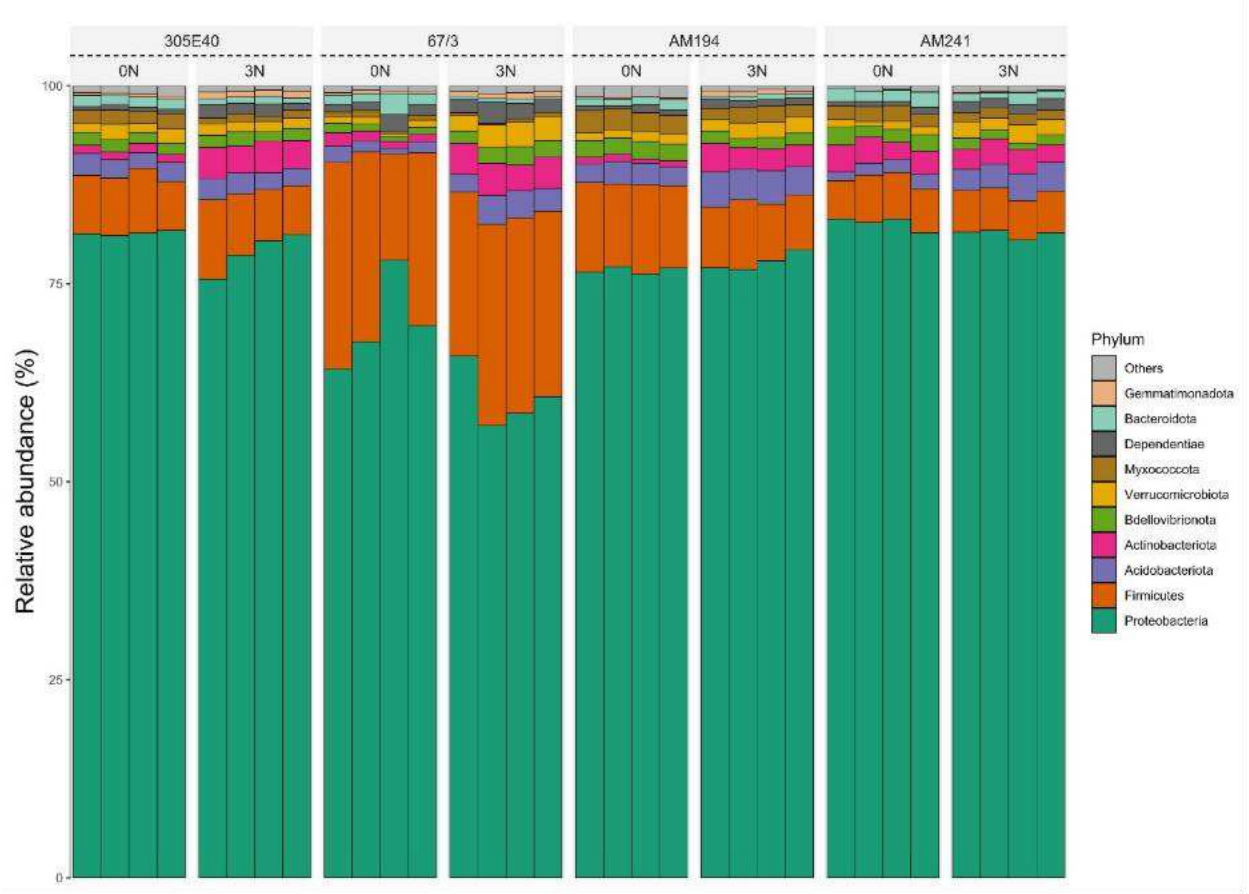


Figure 5. Relative abundance of dominant bacterial phyla across genotypes and treatments. Bar plot showing the top 10 most abundant phyla based on relative abundance. Taxa are displayed as proportions of total reads per sample. Bars represent mean relative abundance across samples within each group. Phyla outside the top 10 are grouped as “Others.”

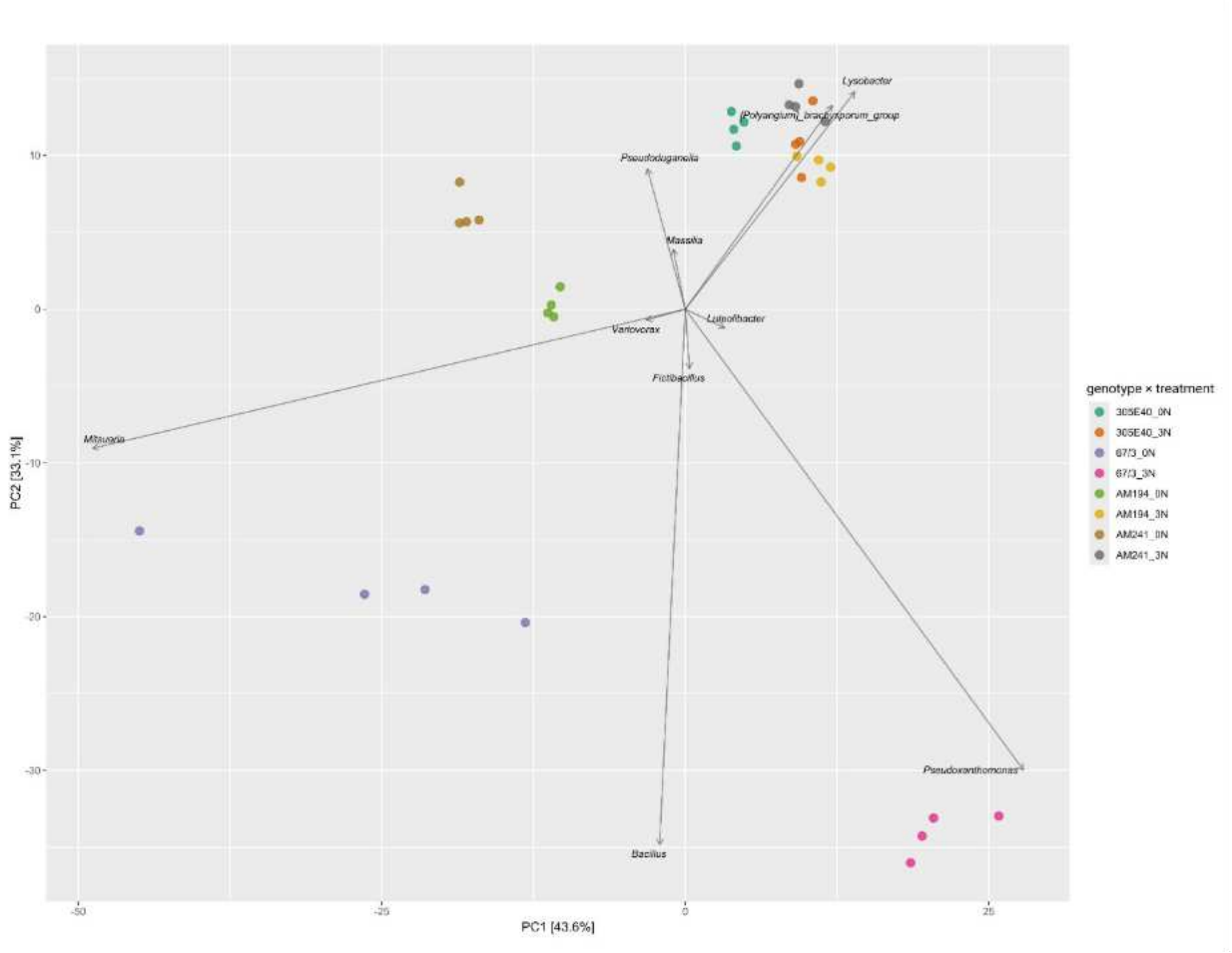


Figure 6. PCA biplot of taxonomic composition aggregated at the *Genus* level. Samples are colored by genotype × treatment group. Arrows represent taxa loadings, indicating taxa contributing most to the ordination structure.

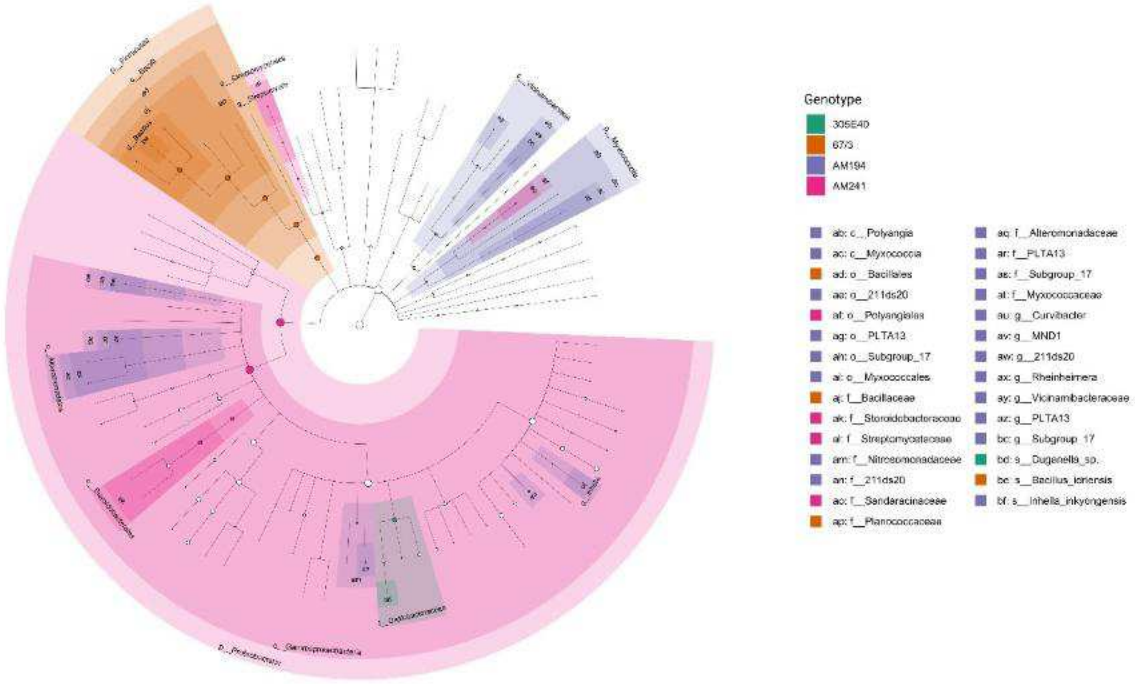


Figure 7. LEfSe cladogram showing taxonomic lineages differentially enriched between genotypes (305E40, Green; 67/3, Orange; AM194, Purple; AM241, Pink). Nodes represent taxa significantly associated with each genotype.

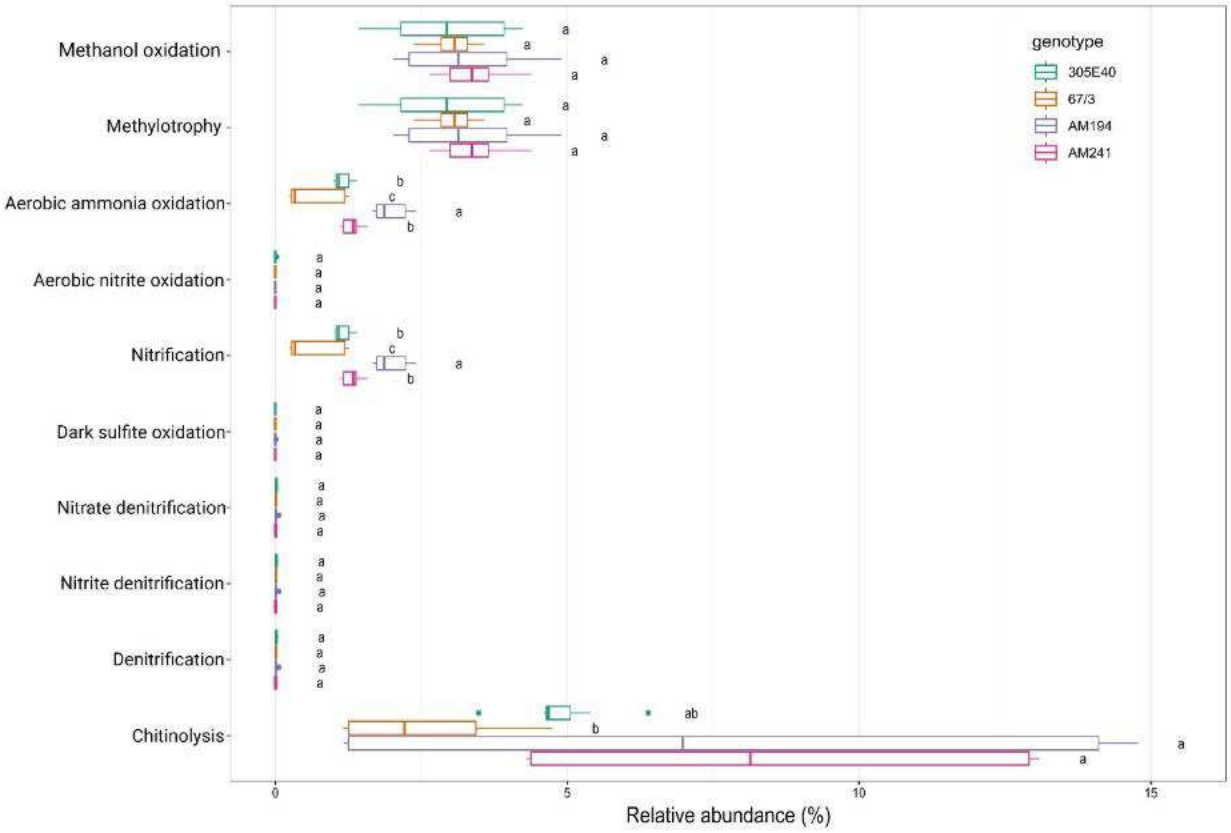


Figure 8 – Putative microbial functional groups were inferred from 16S rRNA gene amplicon sequence variants using the microeco implementation of the FAPROTAX database. Functional annotations were calculated from taxonomic assignments and expressed as abundance-weighted relative abundances (%). Boxplots show the distribution of predicted functional groups across samples for each genotype (305E40, 67/3, AM194, and AM241). Differences among genotypes were assessed using one-way ANOVA. Different letters indicate statistically significant differences between genotypes ($p < 0.05$). Boxes represent the interquartile range, horizontal lines indicate medians, and whiskers represent 1.5 × the interquartile range.

Supplementary Files

This is a list of supplementary files associated with this preprint. Click to download.

- Supplementarymaterial.pdf